On the accuracy of different boundary integral formulations for dielectric bodies using RWG and BC functions
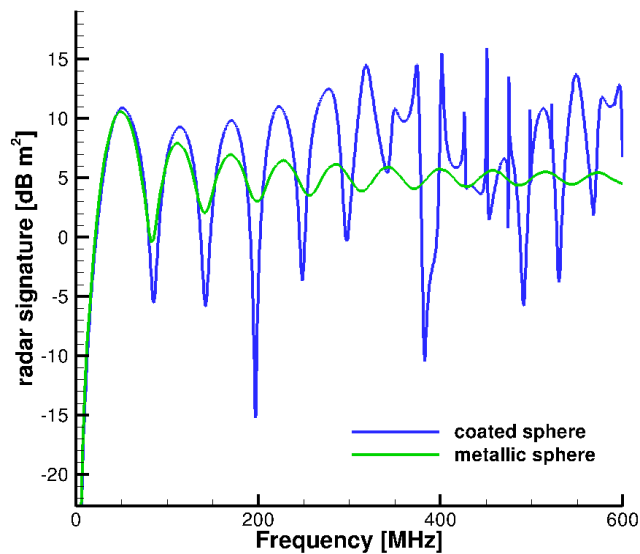
H. van der Ven, C.A. Liontas, K. Cools and D.R. van der Heul

Executive summary

On the accuracy of different boundary integral formulations for dielectric bodies using RWG and BC functions

Report no.
NLR-TP-2015-268

Author(s)
H. van der Ven
C.A. Liontas
K. Cools
D.R. van der Heul

Report classification
UNCLASSIFIED

Date
August 2016

Knowledge area(s)
Computational Physics and
Theoretical Aerodynamics

Descriptor(s)
radar cross section
composites
dielectric
numerical methods

Problem area

Radar cross-section prediction methods are a welcome addition to experimental ways of ascertaining the radar cross-section of aircraft. In previous projects NLR has developed a prediction method for the radar signature of metallic fighter aircraft, possibly equipped with radar absorbing coating. With the advent of composite aircraft, such as modern fighter aircraft and RPAS, radar cross-section prediction methods must also be able to model the dielectric nature of composites. Composites are primarily applied to reduce the weight of the aircraft, but may also be used as radar-absorbing structures.

The most accurate radar cross-section prediction methods are based on the so-called integral equations which describe the electric and magnetic currents on a scatterer illuminated by a radar wave. There exist several formulations for the integral equations describing the scattering of dielectric bodies in literature. The advantages and disadvantages of the different formulations are not always clear. A wrong choice may result in inaccurate predictions and/or long computing times. The current paper investigates the accuracy of various formulations and their discretization, but also takes the efficiency of the formulations into account.

This report is based on a manuscript submitted to IEEE Transaction on Antennas and Propagation.

On the accuracy of different boundary integral formulations for dielectric bodies using RWG and BC functions

Description of work

The two most popular formulations are the PMCHWT and Müller formulations. The first is accurate but difficult to solve, and the second is less accurate, but more easy to solve. Recent developments in finite element theory have improved the accuracy of the second formulation by changing the testing procedure. The usual, so-called, RWG test functions (which are also used to expand the currents) are replaced by so-called BC functions.

The current paper compares the PMCHWT and Müller formulations (amongst others), tested with either RWG or BC functions. Moreover, it is investigated whether the BC functions can also be used to expand the magnetic current.

The different formulations are rigorously compared on two canonical objects with low contrast. The formulations are evaluated on their order of accuracy, error, and condition number.

Results and conclusions

The different formulations have comparable performance on smooth objects, but behave quite differently on non-smooth objects. The formulations which use BC functions to expand the currents lose two orders of accuracy. Both the classical PMCHWT and Müller formulation lose one order. The modern Müller formulation using BC functions as testers maintains its second order of accuracy on non-smooth objects.

Hence, the modern Müller formulation performs best in terms of accuracy for low-contrast dielectric bodies.

Applicability

The radar cross-section prediction tool based on the modern Müller formulation will be able to predict the radar signature of modern fighter aircraft and RPAS.

In particular, the prediction tool can model objects consisting of perfectly electrically conducting surfaces, various layers of dielectric material, and/or radar-absorbing materials.

On the accuracy of different boundary integral formulations for dielectric bodies using RWG and BC functions

H. van der Ven, C.A. Liontas[1], K. Cools[2] and D.R. van der Heul[3]
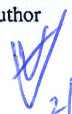
[1] Fraunhofer Institut

[2] University of Nottingham
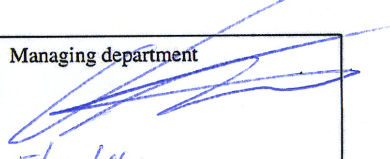
[3] University of Delft

Customer	National Aerospace Laboratory NLR
Contract number	-----
Owner	NLR
Division NLR	Aerospace Vehicles
Distribution	Unlimited
Classification of title	Unclassified
Date	August 2016

Approved by:

Author	Reviewer	Managing department
2/12/2016	J hansinh Rotger inh 31/10	5/12/16

Contents

This page is intentionally left blank.

1 Introduction

The computation of the frequency domain electromagnetic field scattered by a PEC object, as the solution of a discretized boundary integral equation, used to be relatively straightforward. One chooses a linear combination of the electric field integral equation (EFIE) and the magnetic field integral equation (MFIE) formulation of the problem and a Galerkin finite element discretisation based on an expansion of the electric current distribution in RWG basis functions. Deciding on the balance between MFIE and EFIE is a trade-off between efficiency of the solution algorithm and the accuracy of the solution obtained. A better understanding of the properties of the MFIE operator revolutionized this approach with the introduction of an alternative set of test functions by Buffa and Christiansen (Ref. 2). Using conformal testing, the accuracy of the discretisation of the MFIE can be made comparable to that of the EFIE, without affecting its more favorable properties for iterative solution (Ref. 4).

On the other hand, a plethora of algorithms can be constructed to compute the electromagnetic field scattered by a dielectric object. Considerations are the choices for the basis and testing functions and how the integral equations, the EFIE and MFIE for the different media, are combined.

This discretisation should lead to a linear system of equations that can be solved efficiently and accurately for a unique solution, for any meaningful excitation. This means the resulting matrix should be square, have a moderate condition number, and be of full rank for every frequency of the excitation. Because the matrix is not (necessarily) normal, the eigenvalue spectrum, the condition number or the spectral condition number can not give conclusive information on the efficiency the system can be solved with using an iterative method for general matrices, e.g. GMRES. This is analysed in the milestone paper by Greenbaum (Ref. 5) and also observed in the experiments presented in (Ref. 16, 13).

In terms of accuracy, not only the order is important but also the norm in which the error is measured. For electromagnetic scattering problems it is the energy norm that is relevant and it is with respect to this norm that the discretisation is required to fulfill an inf-sup condition in order to guarantee optimal convergence. This property will guarantee that the physical energy in the approximation error will be small when a sufficiently large number of degrees of freedom are being used. Finally, those formulations are preferred that do not require the discretisation of line integrals but only of surface integrals, and allow modelling of *composite* objects, that is, discretisation of the surface currents on interface surfaces where more than two materials meet.

Originally, boundary integral equations (BIE) for dielectric scatterers were based on the now classic formulations of the the PMCHW(T) (Ref. 10), the Müller (Ref. 11) equations, and CFIE ((Ref. 15) and references therein), and combined with either RWG or rotated RWG basis-functions for expansion of both electric and magnetic current. An illustrative comparison of these formulations is presented in Jung et al. (Ref. 6, 7). By combining the EFIE and MFIE directly or in their rotated form, sixteen different formulations of the CFIE can be formulated. These are assessed based on the accuracy of the current distribution and scattered field for a dielectric sphere, cube and cylinder using linear combinations of RWG and rotated RWG functions for testing and expansion of the current distributions. Jung et al. show that combining the EFIE and MFIE does not necessarily suppress interior resonances, and some combinations do not converge.

How the specific linear combination affects the convergence of the iterative solvers that are used to solve the resulting linear system is addressed in Ylä-Oijala et al. (Ref. 13). Like in the case of PEC scatterers, Fredholm equations of the first kind lead to accurate solutions but also to linear systems that are computationally intensive to invert, while Fredholm equations of the second kind can not meet the accuracy of the former, especially for nonsmooth scatterers and/or high contrast testcases, but generally give rise to linear systems of equations that can be significantly more efficiently solved. The accuracy of the latter is improved in (Ref. 16) by replacing the RWG basis functions by Trintinalia-Ling (Ref. 8) basis functions, and in (Ref. 14) by replacing the RWG test functions by (rotated) Buffa-Christiansen (Ref. 2) test functions without jeopardizing the favorable properties of the resulting linear systems. An alternative based on the use of pulse basis functions is presented in (Ref. 9). Although the theory behind the use of BC functions as test functions for the MFIE or Müller formulations is not complete, an important aspect is that the BC functions are in the dual of the range of integral operator (Ref. 14, 12).

In Ylä-Oijala et al.(Ref. 12) the use of dual *basis* functions in BIEs has been introduced in a broader expoloration of all the possible combinations of disrcetizations using RWG and BC as basis functions, and (rotated) RWG and BC as test functions. The main objective of the paper was to experimentally establish the claim that the test space should be in the dual of the range. The use of BC functions as basis functions was not explored in depth, whereas the resulting discretizations may have some desirable properties.

The current paper investigates the use of BC functions as basis functions in more detail, and compares the resulting discretizations with state-of-the-art discretizations for dielectric bodies. First, the performance of BC functions as interpolators is investigated numerically, establishing the order of accuracy of the interpolation. It is demonstrated that the interpolation errors of

BC functions are not as high as predicted by generally valid upper bounds. Second, with rigorous grid convergence studies the order of accuracy of different boundary integral formulation for smooth and non-smooth objects of low contrast is determined. The condition numbers of the system matrices is reported, as a first indication how efficiently the system can be solved. It is shown that the formulations combining RWG and BC as basis functions demonstrate favourable properties of the resulting system matrix, but their order of accuracy is lower than of the other methods, which only use RWG as basis functions. The Müller formulation tested with BC functions, as first introduced by Yan et al. (Ref. 14), provides the best choice, both in terms of accuracy and conditioning.

2 Different boundary integral formulations for dielectric bodies

For homogeneous dielectric materials both the electric current $\boldsymbol{J}_s$ and the magnetic current $\boldsymbol{M}_s$ are unknowns, and in order to obtain sufficient equations, one has to consider the EFIE, resp. MFIE, in both media:

$$
\begin{aligned}
4\pi \boldsymbol{E}_t^{\text{inc}} &= \eta_1 \boldsymbol{L}^1(\boldsymbol{J}_s) + \boldsymbol{K}^1(\boldsymbol{M}_s) \\
4\pi \eta_1 \boldsymbol{H}_t^{\text{inc}} &= \boldsymbol{L}^1(\boldsymbol{M}_s) - \eta_1 \boldsymbol{K}^1(\boldsymbol{J}_s) \\
0 &= \eta_2 \boldsymbol{L}^2(\boldsymbol{J}_s) + \boldsymbol{K}^2(\boldsymbol{M}_s) \\
0 &= \boldsymbol{L}^2(\boldsymbol{M}_s) - \eta_2 \boldsymbol{K}^2(\boldsymbol{J}_s),
\end{aligned}
$$

where η_1 is the impedance of the exterior medium and η_2 the impedance of the dielectric. The operators $\boldsymbol{L}^i$ and $\boldsymbol{K}^i$ are the integral operators acting on a tangential vector field $\boldsymbol{X}$:

$$
\boldsymbol{L}^i(\boldsymbol{X}) = jk^i \left(\int_S \left(\boldsymbol{X}\phi - \frac{1}{(k^i)^2}(\nabla' \cdot \boldsymbol{X})\nabla'\phi \right) d\boldsymbol{r}' \right)_t, \tag{1}
$$

$$
\boldsymbol{K}^i(\boldsymbol{X}) = \left(\oint_S \boldsymbol{X} \times \nabla'\phi d\boldsymbol{r}' \right)_t + 2\pi \boldsymbol{n}^i \times \boldsymbol{X}, \tag{2}
$$

where k^i is the wavenumber in medium i, $\phi = e^{-jkR}/R$ the free space Green's function ($R = |\boldsymbol{r} - \boldsymbol{r}'|$), the normal $\boldsymbol{n}^i$ on the surface S points into medium i (so $\boldsymbol{n}^2 = -\boldsymbol{n}^1$), and the subscript t refers to the tangential part of the vector field.

The first two equations are a condition on a pair of currents $(\boldsymbol{J}, \boldsymbol{M})$ to be the traces of solutions of the exterior Maxwell equations. Similarly, the last two equations are fulfilled by any pair of

currents that are the traces of solutions to the interior Maxwell equations. As such, neither the first two nor the last two can be solved uniquely in isolation from the other pair. This is a consequence of the physical fact that solving the transmission problem requires knowledge of the interior of the object.

In order to arrive at a set of equations that can be uniquely solved, certain linear combinations of the exterior and interior equations need to be taken. Some of the most popular choices are briefly revisited in the next paragraphs.

As explained in the introduction, we will be considering different formulations in the integral formulation, different basis functions, and different testers used for the equations. Therefore the integral equations will be formulated in the weak sense, including the test functions. In the following, the EFIE will be tested with either RWG or $n \times$RWG test functions, where the first choice is conforming. The two formulations will be denoted by T-EFIE, resp. N-EFIE. The MFIE will be tested with either RWG, $n \times$RWG, or BC functions. These three formulations will be denoted by T-MFIE, N-MFIE, and W-MFIE (W for well-tested). For PEC scatterers it is known (Ref. 4) that T-MFIE is conforming (and unstable), N-MFIE is well conditioned, and W-MFIE is both conforming, stable and well conditioned. With a stable discretization we mean that the absolute value of the diagonal entry of the system matrix is greater than the off-diagonal entries (note that this is not the same as diagonally dominant, which means that the absolute value of the diagonal entry is greater than the *sum* of the absolute values of the off-diagonal entries). Stability of a discretization is beneficial for the performance of linear solvers, but in general not equivalent to a good condition number(Ref. 5).

For an integral operator X mapping the space of divergence conforming vector fields to curl conforming vector fiels denote

$$X_{hh'} = \langle h, X(h') \rangle,$$

for h, h' in the divergence conforming function space. In this notation, the system matrix of EFIE discretized with RWG functions for a PEC scatterer is

$$(L_{f_e f_{e'}})_{ee'},$$

for the edges e, e' of the mesh. Here, and in the following, $\boldsymbol{f}_e$ will be the RWG function defined on edge e, and $\boldsymbol{g}_e$ the BC function. We will use the shorthand L_{ff} for the matrix $(L_{f_e f_{e'}})_{ee'}$. Similarly, the system matrix of W-MFIE for a PEC scatterer is denoted by K_{gf}: the current is expanded in RWG functions and MFIE is tested with BC functions. The system matrix of N-MFIE for PEC is denoted by K_{nf}: the MFIE is tested with $\boldsymbol{n} \times$RWG. From Cools et al. (Ref. 4) we

know that the system matrices L_{ff}, L_{gg}, K_{gf} and K_{fg} are stable and obtained from a conforming testing procedure. (It should be noted that L_{ff} and L_{gg} are not well conditioned; Calderon preconditioning (Ref. 1) can improve the conditioning of these matrices).

The classical PMCHWT formulation, denoted by T-PMCHWT in this paper, solves the following discretized equations:

$$\begin{pmatrix} \eta_1 L_{ff}^1 + \eta_2 L_{ff}^2 & K_{ff}^1 + K_{ff}^2 \\ -(K_{ff}^1 + K_{ff}^2) & L_{ff}^1/\eta_1 + L_{ff}^2/\eta_2 \end{pmatrix} \begin{pmatrix} \boldsymbol{j} \\ \boldsymbol{m} \end{pmatrix}$$

$$= \begin{pmatrix} \langle \boldsymbol{f}_e, 4\pi \boldsymbol{E}_t^{\mathrm{inc}} \rangle_e \\ \langle \boldsymbol{f}_e, 4\pi \boldsymbol{H}_t^{\mathrm{inc}} \rangle_e \end{pmatrix}, \tag{3}$$

where $\boldsymbol{j}$, resp. $\boldsymbol{m}$, are the expansion coefficients of the electric current $\boldsymbol{J}_h = \sum_e j_e \boldsymbol{f}_e$, resp. of the magnetic current $\boldsymbol{M}_h = \sum_e m_e \boldsymbol{f}_e$. The identity-like terms in the K-operators cancel each other (since the normals have opposite sign), ensuring that the hypersingular terms of the L-operators dominate the system matrix. Hence, the T-PMCHWT is a stable formulation (Ref. 3).

The classical N-Müller formulation solves the following discretized equations:

$$\begin{pmatrix} -K_{nf}^1 - \mu_r K_{nf}^2 & L_{nf}^1 + \frac{k_2}{k_1} L_{nf}^2 \\ L_{nf}^1 + \frac{k_2}{k_1} L_{nf}^2 & K_{nf}^1 + \varepsilon_r K_{nf}^2 \end{pmatrix} \begin{pmatrix} \boldsymbol{j} \\ \boldsymbol{m}/\eta_1 \end{pmatrix}$$

$$= \begin{pmatrix} \langle \boldsymbol{n}^1 \times \boldsymbol{f}_e, 4\pi \boldsymbol{H}_t^{\mathrm{inc}} \rangle_e \\ \langle \boldsymbol{n}^1 \times \boldsymbol{f}_e, \frac{4\pi}{\eta_1} \boldsymbol{E}_t^{\mathrm{inc}} \rangle_e \end{pmatrix}. \tag{4}$$

The hypersingular terms of the L-operators cancel each other, ensuring that the identity-like terms in the K operators dominate the system matrix (the normal in the test functions are medium-specific). So N-Müller is stable, but suffers from the same accuracy issues as N-MFIE for PEC and tends to yield results that lack in accuracy compared to the EFIE, especially in the presence of non-smooth geometries.

The modern Müller formulation of Yan et al. (Ref. 14), denoted by W-Müller in this paper, replaces the $\boldsymbol{n} \times$RWG test functions with BC functions to obtain:

$$\begin{pmatrix} -K_{gf}^1 + \mu_r K_{gf}^2 & L_{gf}^1 - \frac{k_2}{k_1} L_{gf}^2 \\ L_{gf}^1 - \frac{k_2}{k_1} L_{gf}^2 & K_{gf}^1 - \varepsilon_r K_{gf}^2 \end{pmatrix} \begin{pmatrix} \boldsymbol{j} \\ \boldsymbol{m}/\eta_1 \end{pmatrix}$$

$$= \begin{pmatrix} \langle \boldsymbol{g}_e, 4\pi \boldsymbol{H}_t^{\mathrm{inc}} \rangle_e \\ \langle \boldsymbol{g}_e, \frac{4\pi}{\eta_1} \boldsymbol{E}_t^{\mathrm{inc}} \rangle_e \end{pmatrix}. \tag{5}$$

As demonstrated by Yan et al., the W-Müller formulation improves the accuracy compared to that of N-Müller.

Although the diagonal blocks of T-PMCHWT and W-Müller contain the well-tested and stable system matrices L_{ff} and K_{gf}, the off-diagonal blocks are not well-tested. This may have a negative effect on the accuracy of the formulations. In the following, mixed formulations will be presented for which all the four blocks in the systems matrix are well-tested and stable. The mixed formulations use different basis functions for the electric and magnetic current: the electric current is expanded in RWG functions and the magnetic current is expanded in BC functions. The mixed formulations have been first introduced in (Ref. 12).

The mixed formulation of PMCHWT, denoted by M-PMCHWT, is given by:

$$
\begin{pmatrix} \eta_1 L_{ff}^1 + \eta_2 L_{ff}^2 & K_{fg}^1 + K_{fg}^2 \\ -(K_{gf}^1 + K_{gf}^2) & L_{gg}^1/\eta_1 + L_{gg}^2/\eta_2 \end{pmatrix} \begin{pmatrix} \boldsymbol{j} \\ \boldsymbol{m} \end{pmatrix}
$$

$$
= \begin{pmatrix} \langle \boldsymbol{f}_e, 4\pi \boldsymbol{E}_t^{\mathrm{inc}} \rangle_e \\ \langle \boldsymbol{g}_e, 4\pi \boldsymbol{H}_t^{\mathrm{inc}} \rangle_e \end{pmatrix}, \tag{6}
$$

where $\boldsymbol{m}$ is now the vector of expansion coefficients of the magnetic current with respect to BC functions. Note that the first equation is tested with RWG functions, whereas the second is tested with BC functions.

The mixed formulation of Müller, denoted by M-Müller, is given by:

$$
\begin{pmatrix} -K_{gf}^1 + \mu_r K_{gf}^2 & L_{gg}^1 - \frac{k_2}{k_1} L_{gg}^2 \\ L_{ff}^1 - \frac{k_2}{k_1} L_{ff}^2 & K_{fg}^1 - \varepsilon_r K_{fg}^2 \end{pmatrix} \begin{pmatrix} \boldsymbol{j} \\ \boldsymbol{m}/\eta_1 \end{pmatrix}
$$

$$
= \begin{pmatrix} \langle \boldsymbol{g}_i, 4\pi \boldsymbol{H}_t^{\mathrm{inc}} \rangle_i \\ \langle \boldsymbol{f}_i, \frac{4\pi}{\eta_1} \boldsymbol{E}_t^{\mathrm{inc}} \rangle_i \end{pmatrix}. \tag{7}
$$

Note that again different test functions are used for the different equations.

Apart from the above formulations, four other formulations are evaluated in this paper, three existing ones and a new one. The existing ones are CNF, CTF, and JMCFIE of Ylä-Oijala et al. (Ref. 16). All three expand both the electric and magnetic current in RWG functions. Using the notation at the beginning of the section, CTF is defined as

$$
\begin{cases} \frac{1}{\eta_1}\text{T-EFIE}_1 + \frac{1}{\eta_2}\text{T-EFIE}_2 \\ \text{T-MFIE}_1 + \text{T-MFIE}_2; \end{cases} \tag{8}
$$

CNF is defined as

$$\begin{cases} \quad \text{N-EFIE}_1 + \text{N-EFIE}_2 \\ \frac{1}{\eta_1}\text{N-MFIE}_1 + \frac{1}{\eta_2}\text{N-MFIE}_2; \end{cases} \tag{9}$$

and JMCFIE is defined as

$$\begin{cases} \frac{1}{\eta_1}\text{T-EFIE}_1 + \frac{1}{\eta_2}\text{T-EFIE}_2 - \frac{1}{\eta_1}\text{N-MFIE}_1 - \frac{1}{\eta_2}\text{N-MFIE}_2 \\ \quad \text{N-EFIE}_1 + \text{N-EFIE}_2 + \text{T-MFIE}_1 + \text{T-MFIE}_2. \end{cases} \tag{10}$$

The last, new, formulation is a CFIE formulation, denoted by M-CFIE and based on the mixed expansion as used in M-PMCHWT and M-Müller:

$$\begin{pmatrix} \alpha\eta_1 L^1_{ff} + (1-\alpha)\eta_1 K^1_{gf} & \alpha K^1_{fg} - (1-\alpha)L^1_{gg} \\ \alpha\eta_2 L^2_{ff} + (1-\alpha)\eta_2 K^2_{gf} & \alpha K^2_{fg} - (1-\alpha)L^2_{gg} \end{pmatrix} \begin{pmatrix} \boldsymbol{j} \\ \boldsymbol{m} \end{pmatrix}$$

$$= \begin{pmatrix} \alpha\langle \boldsymbol{f}_i, 4\pi \boldsymbol{E}^{\text{inc}}_t \rangle_i - (1-\alpha)\langle \boldsymbol{g}_i, 4\pi\eta_1 \boldsymbol{H}^{\text{inc}}_t \rangle_i \\ 0 \end{pmatrix}. \tag{11}$$

The M-CFIE is a linear combination of M-EFIE and M-MFIE in the weak sense. Note that the diagonal blocks are not dominant in the M-CFIE formulation. Also note that the system matrix of the corresponding W-CFIE, defined as a linear combination of T-EFIE and W-MFIE, contains columns with only the unstable matrices K_{ff} and L_{gf}, turning it useless.

3 Buffa-Christiansen functions as interpolators

In the mixed formulations defined in the previous section, the BC functions are used as basis functions. It is not obvious that the BC functions are good interpolators, on the contrary, there is reason to think they are not. Being defined as a linear combination of RWG functions on the barycentric mesh, the BC functions are not continuous on a triangle. Hence the classical proof for interpolation accuracy using a sufficiently smooth mapping of the triangle to a master element breaks down.

Numerical experiments have been performed to assess the performance of BC functions as interpolators. Let $\boldsymbol{J}$ be an arbitrary tangential, divergence conforming, vector field on the object. Given a mesh, the current can be either expanded in RWG or BC functions, as:

$$\boldsymbol{J} \approx \sum_e j^{RWG}_e \boldsymbol{f}_e, \qquad \boldsymbol{J} \approx \sum_e j^{BC}_e \boldsymbol{g}_e,$$

since both basis functions are divergence conforming. The expansion in basis functions is computed in the weak sense, by testing the above expressions with test functions defined on the same mesh and solving the resulting system. The choice of the test function is determined by two requirements:

- the test function should be in the dual of the divergence conforming function space, that is, the curl conforming function space;
- the resulting system should be well-conditioned.

Examples of curl-conforming test functions are the rotated RWG and BC functions: $\boldsymbol{n}\times$RWG and $\boldsymbol{n}\times$BC. As the system matrices $\langle \boldsymbol{n} \times \boldsymbol{f}_e, \boldsymbol{f}_{e'} \rangle$ and $\langle \boldsymbol{n} \times \boldsymbol{g}_e, \boldsymbol{g}_{e'} \rangle$ are both ill-conditioned, the only options which satisfy both requirements are to test the RWG expansion with $\boldsymbol{n}\times$BC functions, and the BC expansion with $\boldsymbol{n}\times$RWG functions.

In order to investigate the error in the interpolation, a norm on the difference between the exact current and the interpolated current could be taken. We prefer to compute the radar signature from the interpolated current and compare that with the radar signature of the RWG interpolation obtained on a very fine mesh. The main reason for this is that in most applications the radar signature is the quantity of main interest.

Let $\boldsymbol{H}$ be the magnetic field of a plane wave. The function to be interpolated is the electric current defined by the field $\boldsymbol{n} \times \boldsymbol{H}$ restricted to the surface of the scatterer. The magnetic current is set to zero. Two geometries are considered: a sphere and a cube. The sphere has a radius of 1m, the cube a width of 1m, the frequency of the radar wave is 100MHz. The cube is aligned with the coordinate axes and the wave direction of the plane wave corresponds to 10 degrees azimuth and 45 degrees elevation. Polarization is vertical. The first mesh has a mesh width of $\lambda/7$, where λ is the frequency of the radar wave, and the mesh width is halved with each successive mesh. A grid series consisting of six meshes is generated in this way. The farfield radar signature is computed from the interpolated electric current. The error in the farfield radar signature is computed with respect to the signature on the finest, sixth, mesh in the series using the RWG basis functions.

This numerical experiment is comparable to the numerical experiment on the accuracy of the identity operator in Section IV of Yan et al. (Ref. 14). The electric current on the scatterers is the same in both experiments, being the current on a completely transparent scatterer. Yan considers both electric and magnetic current and assesses the accuracy of the numerical discretization by measuring to what extent the farfield signatures of the two currents cancel each other (a completely transparant scatterer induces no scattered field). In the current numerical experiment only the farfield signature of the electric current is considered, which is more strict since errors
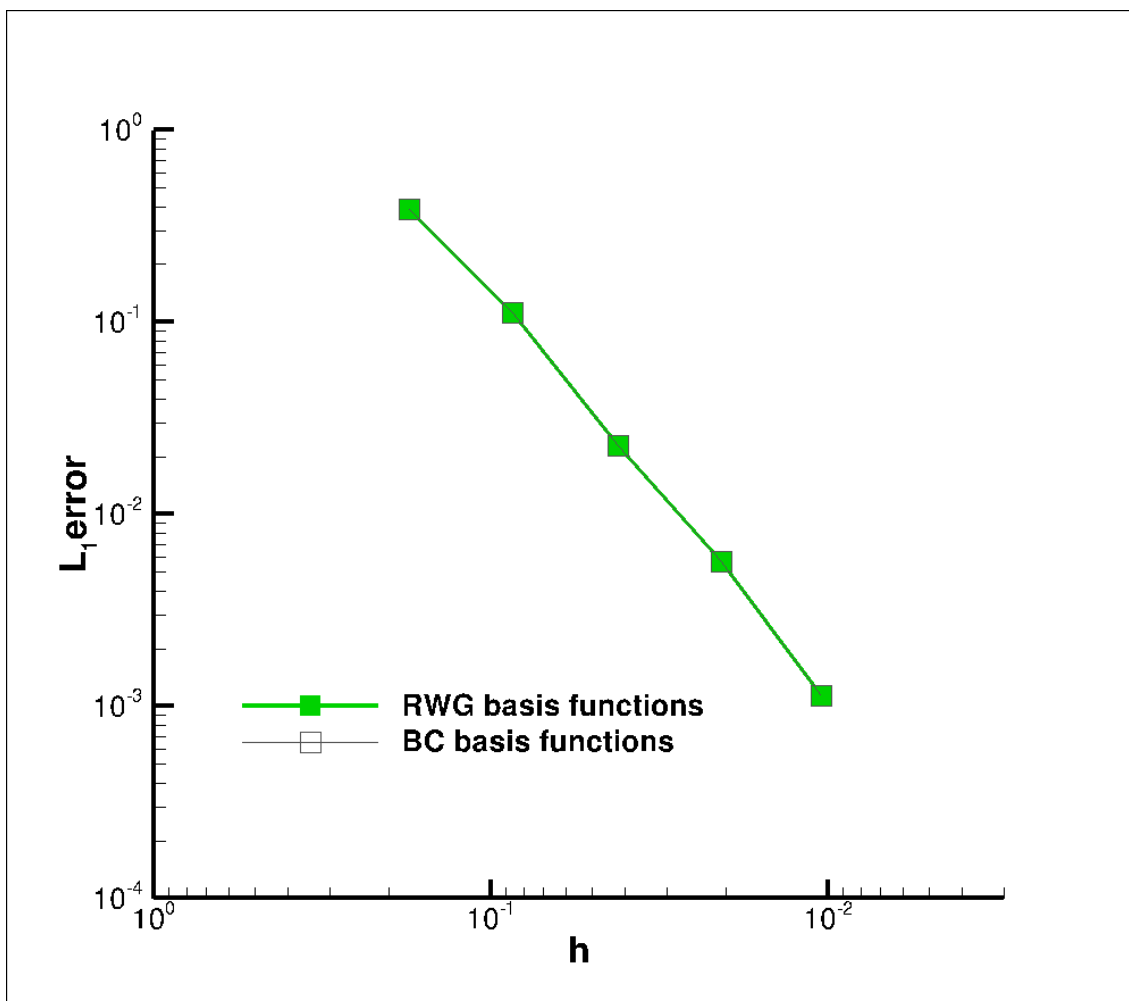
Fig. 1   *Grid convergence in the radar signature of the synthetic current on a sphere. The error is computed as the difference between the solution and the RWG solution obtained on the finest mesh. The errors of the RWG and BC expansions are indistinguishable.*

in electric and magnetic currents cannot cancel each other. Note that Yan used only RWG expansions.

Results are shown in Figure 1 for the sphere and Figure 2 for the cube. For the smooth geometry of the sphere, the RWG and BC expansions are undistinguishable. For the cube, results are different: generally the slope in the error is steeper. The error in the RWG expansion diminishes faster than the error in the BC expansion, but non-smoothly.

The radar signature RCS_h computed from the interpolated current is assumed to satisfy the Richardson interpolation ansatz:

$$\text{RCS}_h = \text{RCS}_{\text{exact}} + Ch^\alpha + O(h^\beta) \qquad (h \to 0),$$
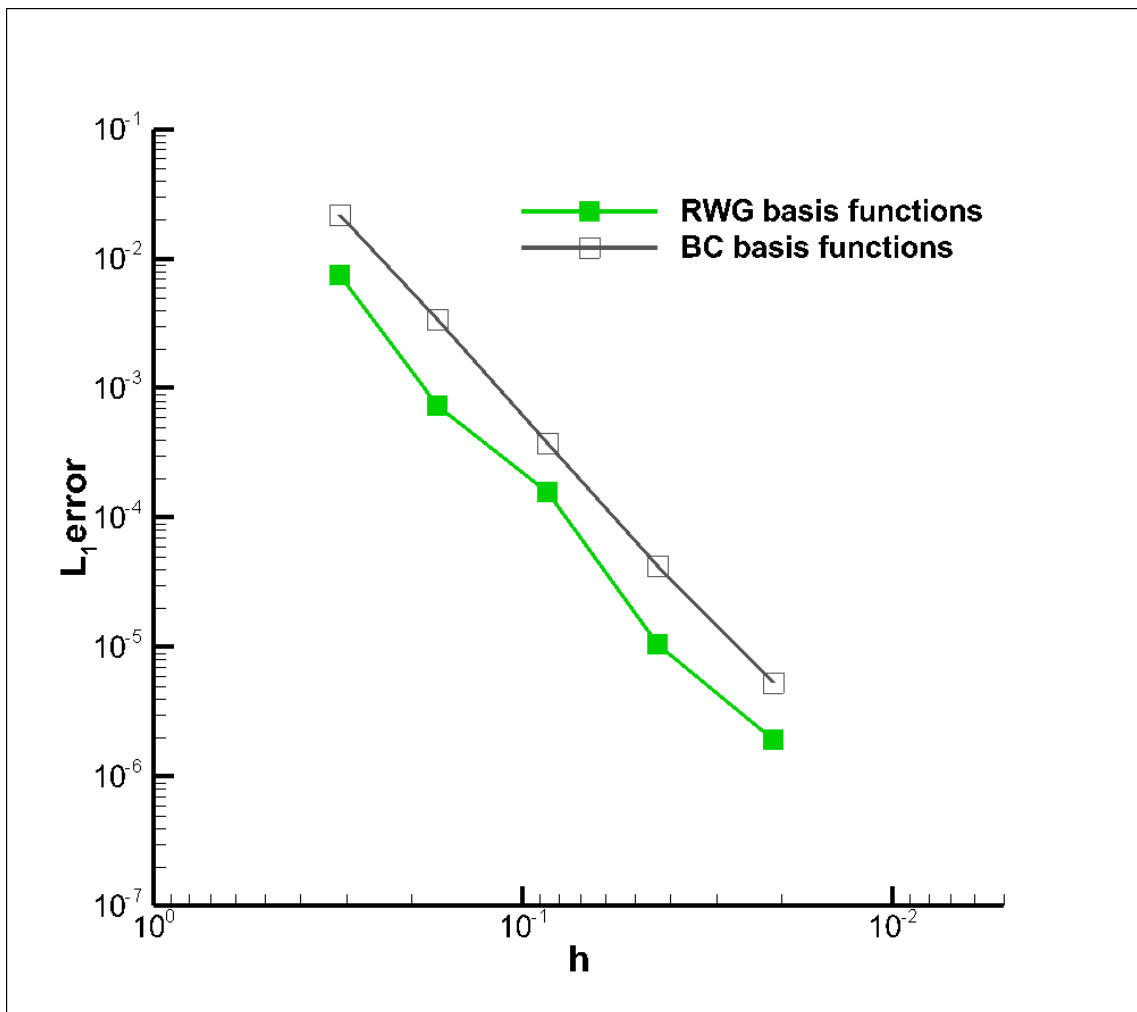
13

Fig. 2   Grid convergence in the radar signature of the synthetic current on a cube. The error is computed as the difference between the solution and the RWG solution obtained on the finest mesh.

14

Table 1   Order of accuracy of the radar signature of a synthetic current

mesh	sphere		cube	
	RWG	BC	RWG	BC
3	1.62	1.62	3.56	2.62
4	2.38	2.38	1.96	3.18
5	1.92	1.92	4.06	3.17
6	1.99	1.99	2.46	3.04

where RCS_{exact} is the exact radar signature from the continuous current, h the mesh width, α the order of accuracy, C the order constant, and $\beta > \alpha$. Neglecting the higher order terms, the Richardson interpolation ansatz contains three unknowns, which can be determined if we compute the discretized radar signature on three different meshes. The orders of accuracy obtained from Richardson interpolation on a successive series of three meshes is shown in Table 1.

For the smooth geometry of the sphere both interpolators shows second order accuracy. For the cube, the order of accuracy is surprisingly third order for the BC expansion, and between second and fourth order for the RWG expansion.

Based on these numerical experiments there is no reason to dismiss the BC functions as interpolators. Their performance is comparable to RWG basis functions.

Remark: The performance of the interpolators depends heavily on the testing procedure. In the above, conformal testing has been applied. Nonconformal testing (RWG expansions tested with RWG functions and BC expansions with BC functions) gives different results: the RWG expansion is second order on both sphere and cube, but the BC expansion fails to converge. This demonstrates that in the design of numerical schemes both basis and test functions should be chosen with care.

4 Results

4.1 Dielectric sphere - frequency sweep

Simulations are performed for a dielectric sphere of radius 1m, $\varepsilon_r = 5$, for a frequency range from 100MHz to 138MHz. So as not to pollute the results with grid effects, different meshes are used for each frequency, each with a mesh width of $\lambda/10$, where λ is the wave length inside the dielectric. Results are compared with the Mie series.
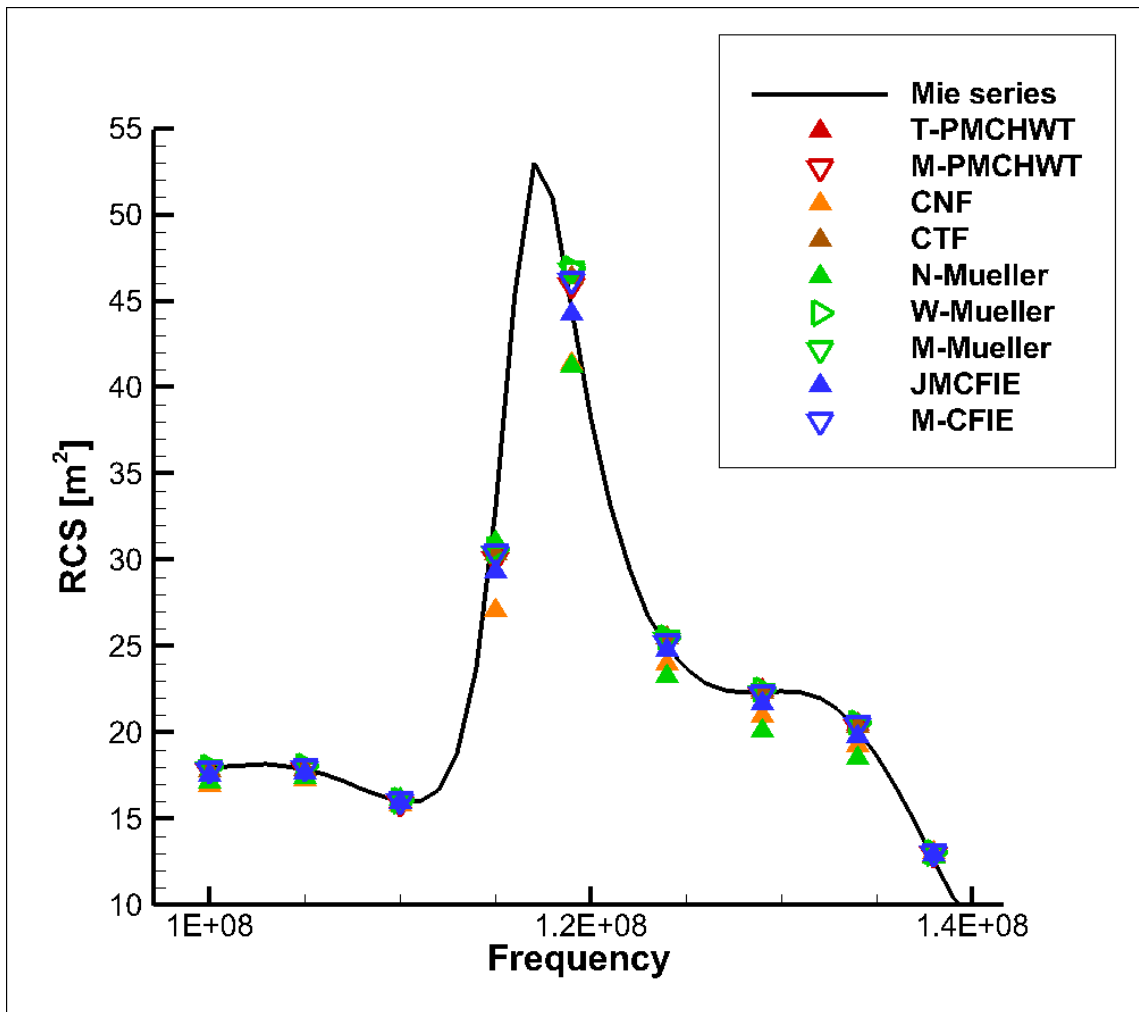
Fig. 3   Radar signature of the dielectric sphere at different frequencies
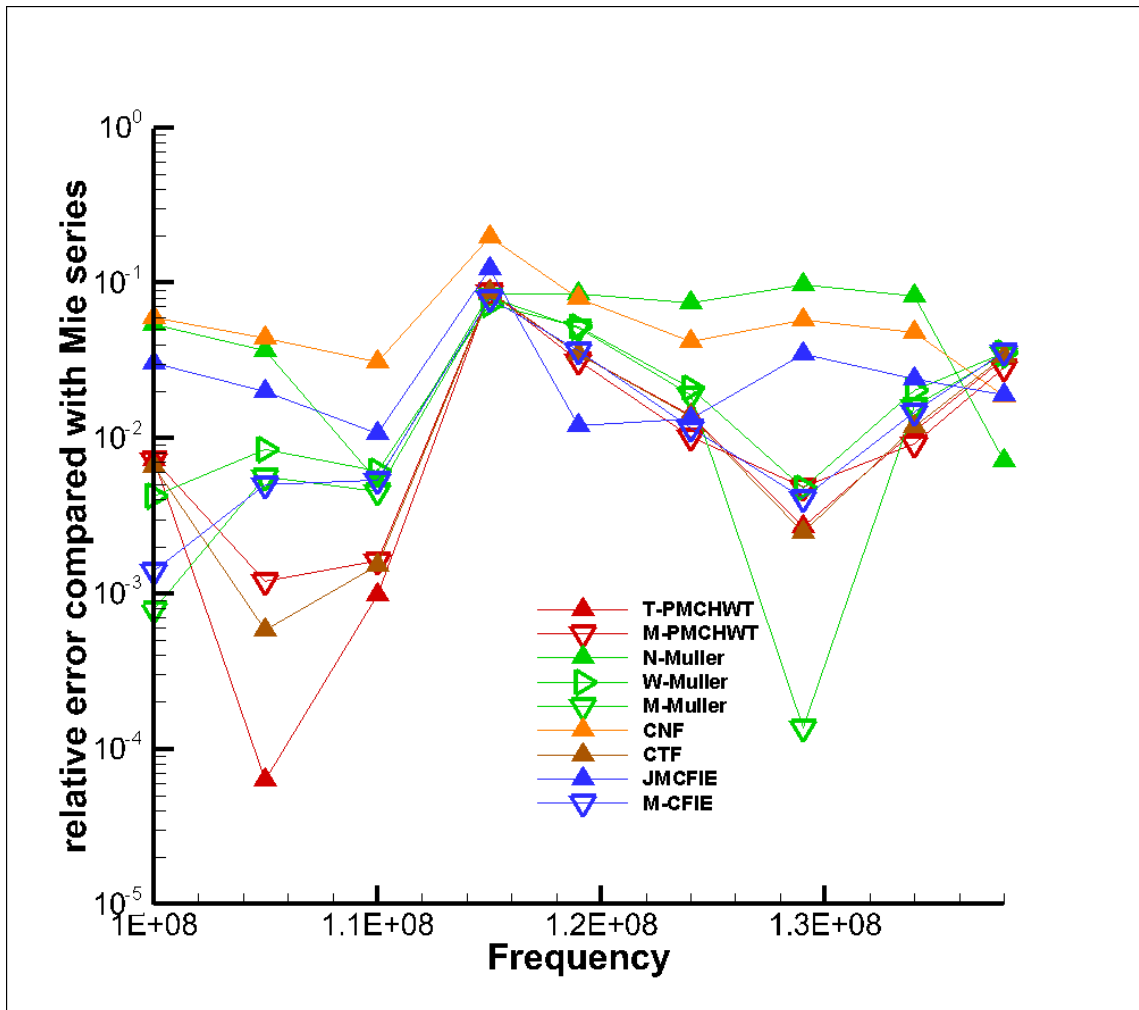
Fig. 4   Error in the radar signature of the dielectric sphere at different frequencies (as compared with the Mie series)
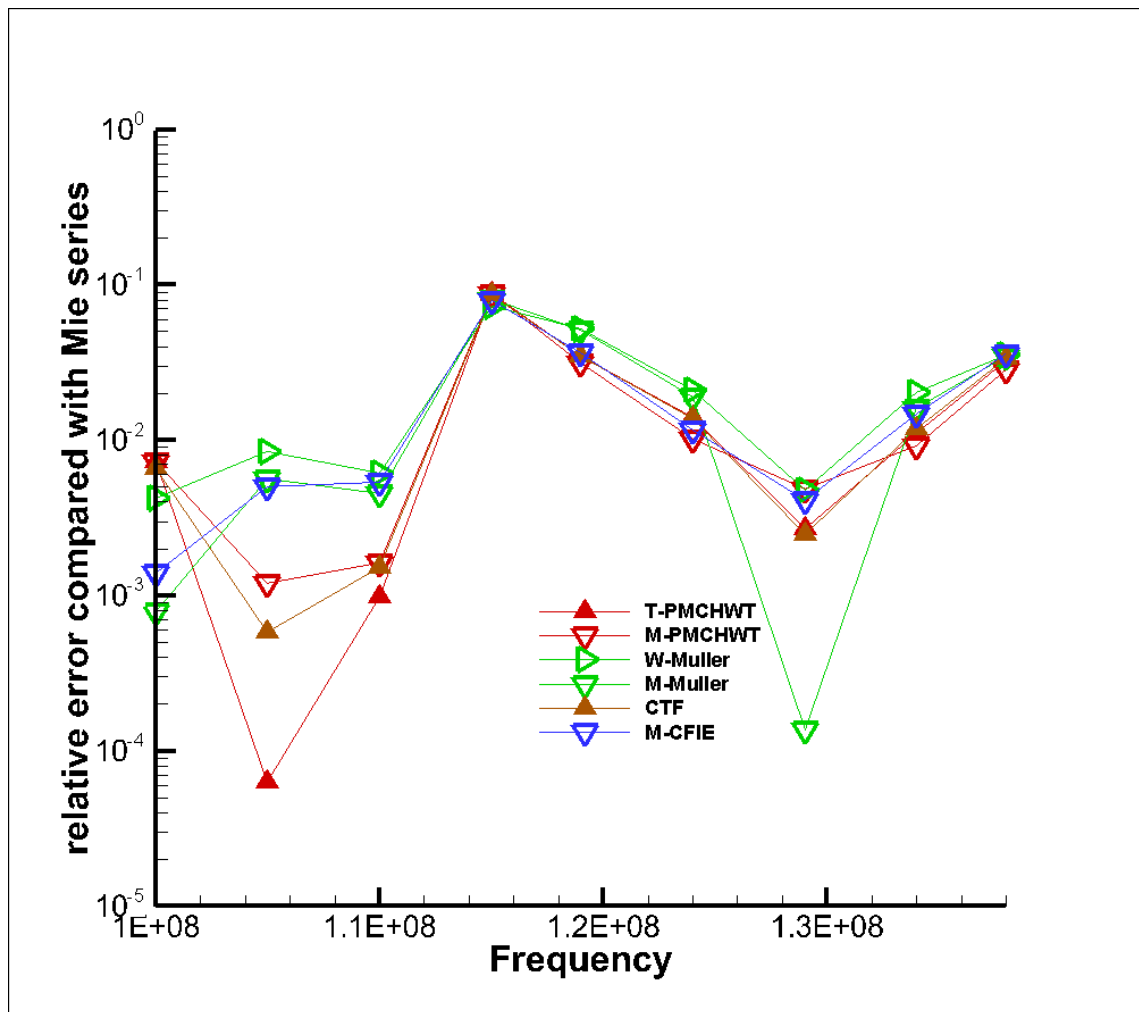
Fig. 5   Error in the radar signature of the dielectric sphere at different frequencies (as compared with the Mie series) for the best performing combinations

Overall results are shown in Figure 3. All methods are capable of predicting, at least qualitatively, the behaviour of the signature as a function of the frequency. There is, however, quite some scatter in the results. The relative error with the Mie series is presented in Figure 4 on a logarithmic scale. Relative errors up to 10% are present. The largest errors occur at the frequency of 115 MHz, where the gradient in the signature is large. The methods CNF, N-Müller, and JMCFIE have the largest errors overall. The results for the other methods are presented (again) in Figure 5 for ease of comparison. Of these six methods, none can be said to be much better than the others.

The condition numbers of the system matrices of the different formulations have been computed. There is little dependence on frequency within the given frequency range, and at this grid refine-

18

ment level there is a little difference between the different formulations. The condition numbers will be discussed in more detail in Section 4.4.

4.2 Dielectric cube - frequency sweep

Simulations are performed for a dielectric cube of width 1m, $\varepsilon_r = 2$, for a frequency range from 100MHz to 350MHz. The cube is aligned with the coordinate axes and the incident plane wave has an azimuth angle of 10 degrees, an elevation angle of 45 degrees, and vertical polarization. So as not to pollute the results with grid effects, different meshes are used for each frequency, each with a mesh width of $\lambda/10$, where λ is the wave length inside the dielectric.

Overall results are shown in Figure 6. All methods predict the same behaviour of the signature as function of the frequency. Note that the signature is on a logarithmic scale. As there is no analytic or reference solution for this case, the grid convergence results of the next sections will be used to evaluate the different formulations.

4.3 Dielectric sphere - grid convergence

Simulations are performed for a dielectric sphere of radius 1m, $\varepsilon_r = 5$, at a frequency of 100MHz on a series of three meshes. The second mesh is the same as used in Section 4.1 for that frequency, the first mesh is once coarsened (about four times less triangles), and the third mesh once refined (about four times more triangles), with respect to this mesh.

As shown in Figure 7 all formulations give convergent results. From the series of three grids, the order of accuracy of the methods can be computed from Richardson interpolation. All methods show at least second order accuracy, apart from maybe N-Müller (see Table 2).

4.4 Dielectric cube - grid convergence

Simulations are performed for a dielectric cube of width 1m, $\varepsilon_r = 2$, at a frequency of 250MHz on a series of three meshes. The second mesh is the same as used in Section 4.2 for that frequency, the first mesh is once coarsened, and the third mesh once refined, with respect to this mesh (as for the sphere).

The results are shown in Figure 8. All formulations give convergent results, but generally at reduced order of accuracy (see Table 2). Only CTF and W-Müller maintain their second order accuracy. The reduction in order of accuracy is the most dramatic for the mixed formulations: the order of accuracy of M-Müller decreases from 2.52 on the sphere to 0.84 on the cube and the M-CFIE results are not even monotone. The cause of the reduction in accuracy for the mixed formulations can be the use of the BC functions as basis functions, which have known issues
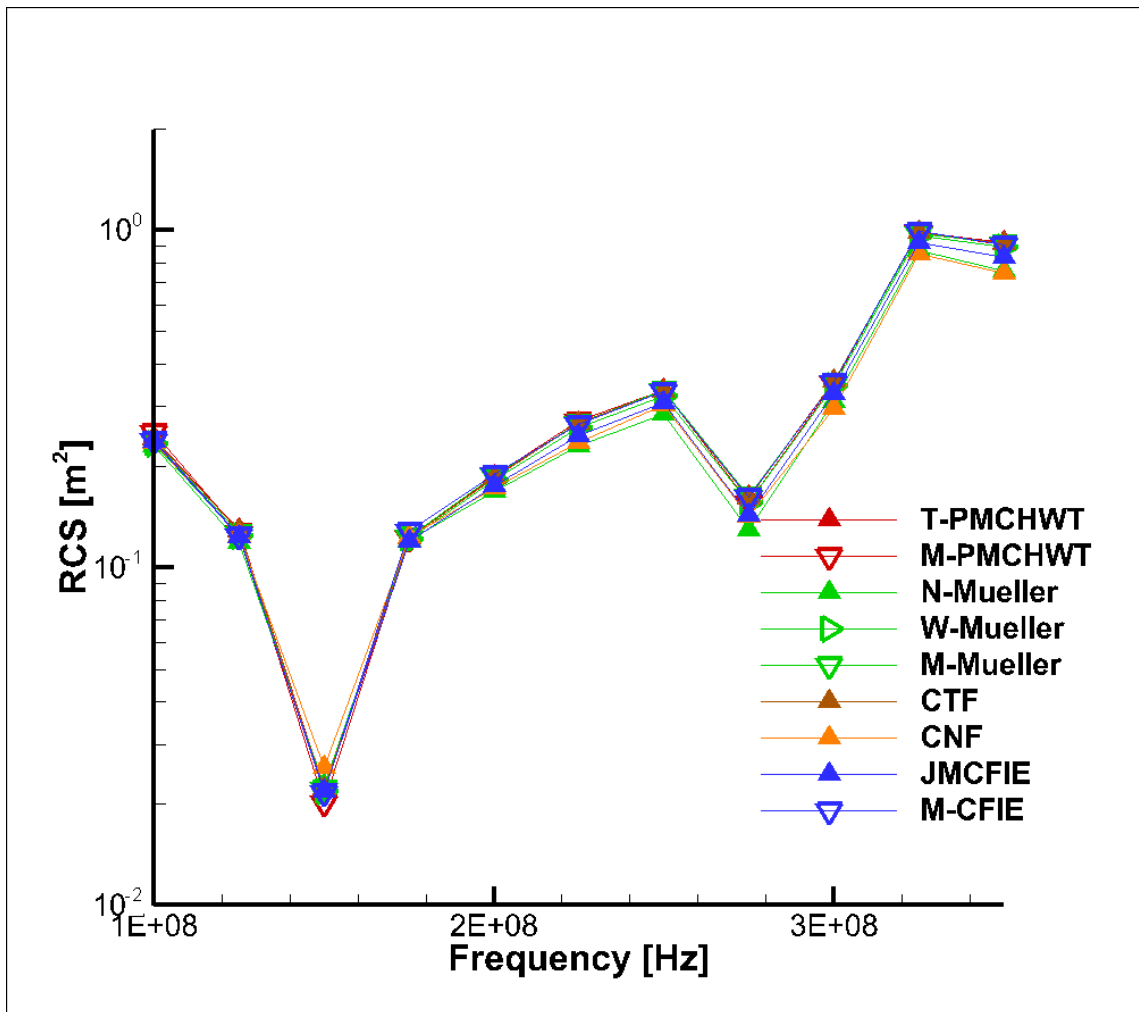
19

Fig. 6   The radar signature of the dielectric cube at different frequencies
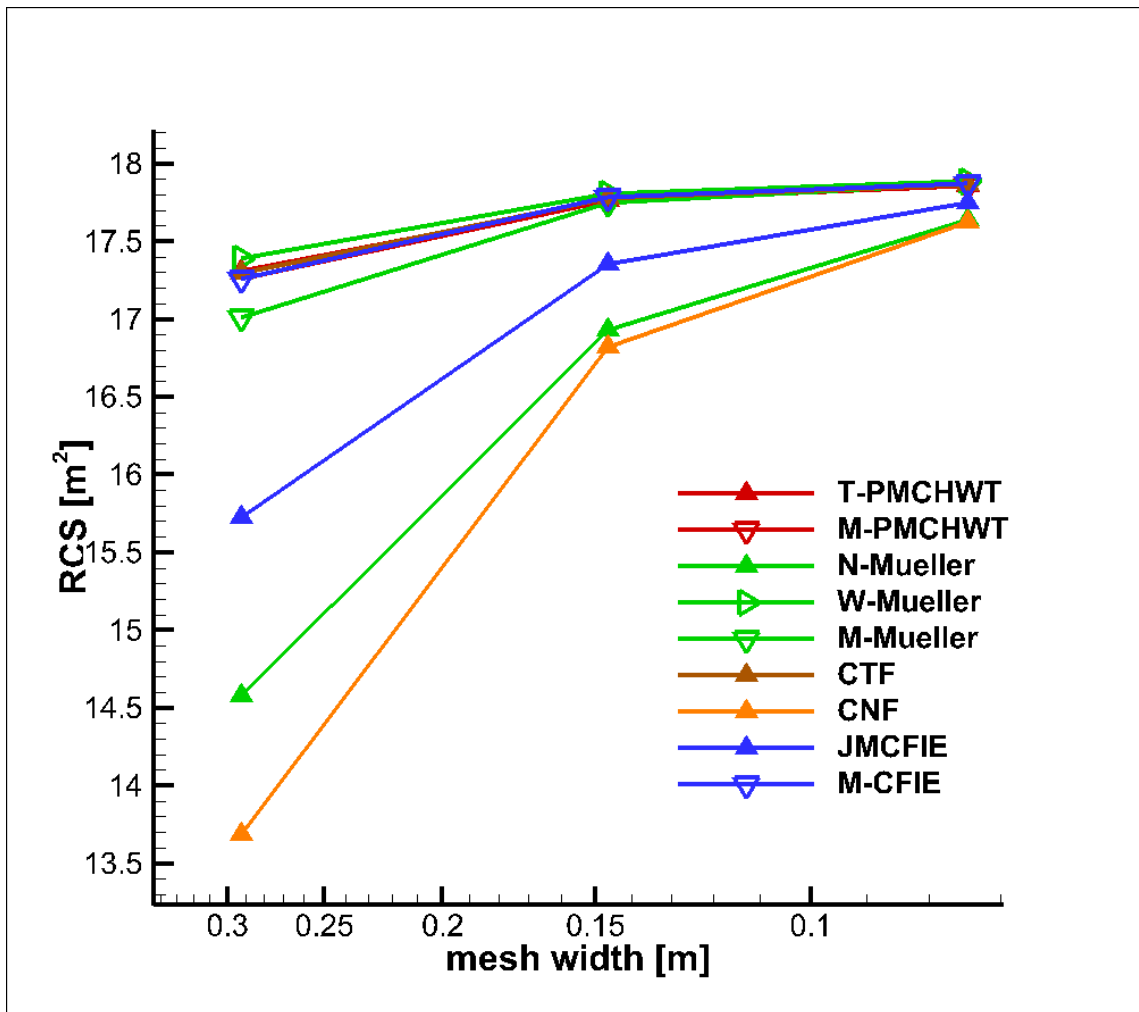
Fig. 7   Grid convergence of the radar signature of the dielectric sphere at 100 MHz

Table 2   Orders of accuracy obtained from the grid convergence studies

method	sphere	cube
T-PMCHWT	2.29	1.39
M-PMCHWT	2.36	0.46
N-Müller	1.73	1.41
W-Müller	2.47	2.57
M-Müller	2.52	0.84
CTF	2.45	2.10
CNF	1.97	1.62
JMCFIE	2.02	1.62
M-CFIE	2.57	n.m.

with sharp edges. On the other hand, this cannot explain the reduction in order of accuracy of the other formulations.

For a given mesh size, the error in the four methods CNF, JMCFIE, N-Müller, and W-Müller, is greater than in the other methods. This is also true for the simulations on the sphere, apart from W-Müller. This means that for these methods a finer mesh is required to reach a given accuracy.

The condition numbers for the grid convergence studies of the sphere, resp. the cube, are tabulated in Table 3, resp. Table 4. The Müller formulations, CNF, and JMCFIE, have comparable condition numbers, which do not increase significantly with grid size. For the other methods the condition number increases with mesh size, but at different rates, with M-PMCHWT scoring the worst. For the classical formulations (which use RWG or $n\times$RWG as testers) it is interesting to see that the methods with the best accuracy (T-PMCHWT and CTF) have increasing condition numbers. As in the PEC case, W-Müller combines accuracy with low condition numbers. Although in general the condition numbers are not good predictors of the number of iterations required for a linear solver to converge (when the matrix is not symmetric or hermitian (Ref. 5)) in this case the condition number relates well with the required number of iterations: the number of GMRES iterations for convergence to a relative residual of 10^{-6} with only a diagonal preconditioner is 25 for M-Müller, 330 for M-CFIE, and 615 for M-PMCHWT, on the medium mesh of the cube.

5   Discussion and conclusions

Different formulations of the discretized integral equations for dielectrics have been compared.

Table 3   Condition numbers for the sphere

method	coarse	medium	fine
T-PMCHWT	47	205	995
M-PMCHWT	179	487	3085
N-Müller	30	39	33
W-Müller	35	31	39
M-Müller	50	44	50
CTF	21	89	430
CNF	15	16	71
JMCFIE	10	16	35
M-CFIE	66	147	484

Table 4   Condition numbers for the cube

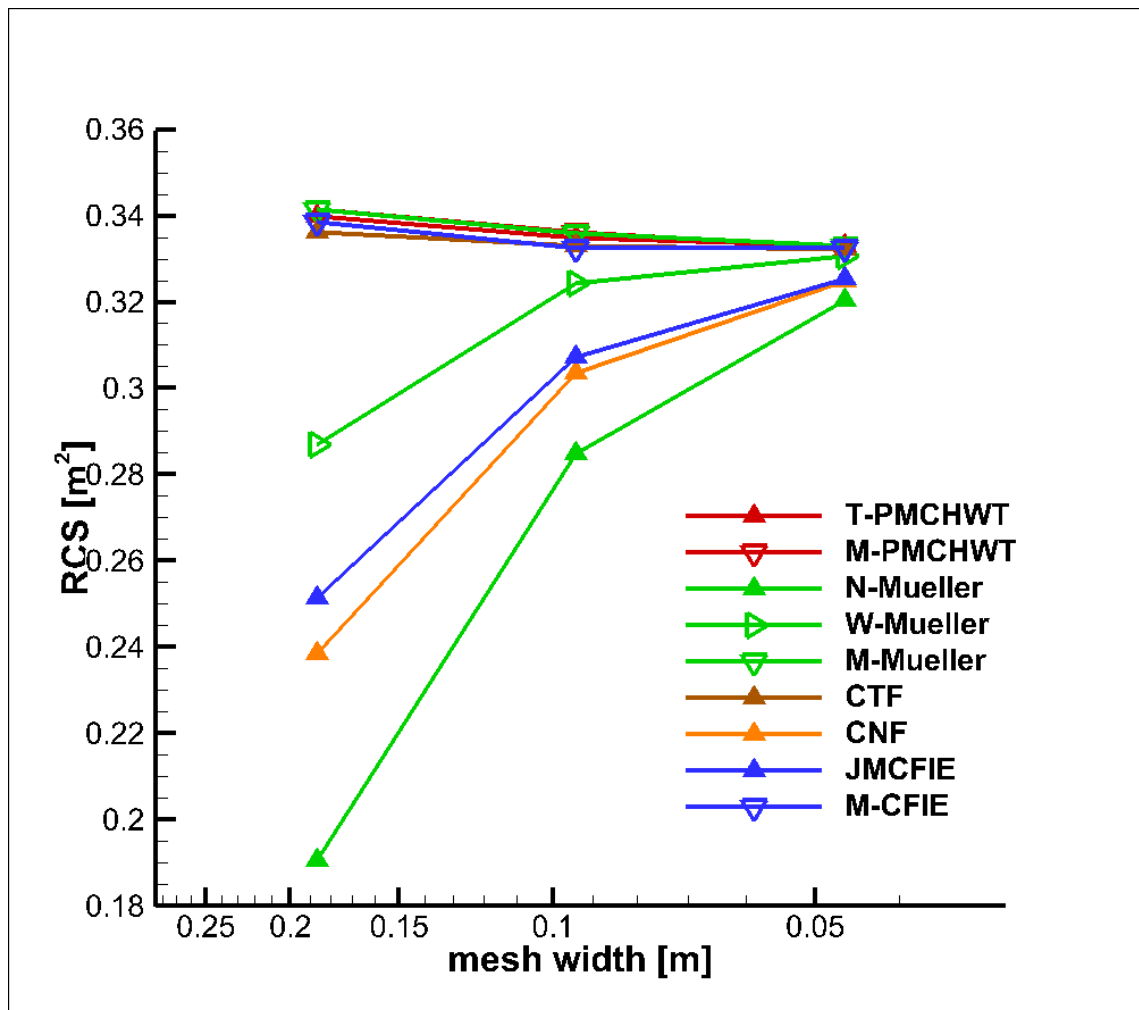| method	coarse	medium	fine
T-PMCHWT	21	84	373
M-PMCHWT	87	223	63000
N-Müller	13	13	11
W-Müller	16	20	17
M-Müller	23	21	20
CTF	16	61	273
CNF	11	11	13
JMCFIE	9	9	19
M-CFIE	63	101	233

Fig. 8   Grid convergence of the radar signature of the dielectric cube at 250 MHz

Of the 'classical' methods which use RWG functions to expand the currents and RWG or rotated RWG functions as testers, CTF performs best in terms of accuracy on the given two geometries. CTF is second order accurate both on the sphere and on the cube, and achieves good results on relatively coarse meshes. T-PMCHWT obtains comparable results but the order of accuracy is lower on the cube. The condition numbers of CTF and T-PMCHWT are relatively large.

The mixed formulations perform equally well as the classical methods on the smooth geometry of the sphere, but their order of accuracy deteriorates more severely on the cube. Most probably, the reduction in order of accuracy is caused by the use of BC functions as interpolators. For non-smooth geometries and especially near the geometric corners the distortion in mapping from a planar regular master element to the local physical element is much larger than in the smooth

24

regions of the object. This may explain the higher impact on using BCs as interpolators on non-smooth geometries.

Based on the results in this paper, the conclusion is that an improved representation of the off-diagonal blocks in the system matrix does not improve the accuracy of the overall method.

The well-tested Müller formulation which uses BC test functions, performs best in terms of order of accuracy and in terms of condition number, both on smooth and non-smooth geometries. The only drawback is that for the cube the error on a given mesh is greater than the error of established methods such as T-PMCHWT and the mixed method M-Müller. In order to establish if this is a consistent feature of W-Müller, more grid convergence studies on non-smooth geometries should be performed.

All-in-all, for low-contrast dielectric bodies, the W-Müller formulation of Yan et al. (Ref. 14) seems the best choice for modelling dielectric bodies, both in terms of accuracy and efficiency.

References

1. F. P. Andriulli, K. Cools, H. Bagci, F. Olyslager, A. Buffa, S. Christiansen, and E. Michielssen. A multiplicative calderon preconditioner for the electric field integral equation. *IEEE Trans. Antennas and Propagat.*, 56(8):2398–2412, 2008.

2. A. Buffa and S.H. Christiansen. A dual finite element complex on the barycentric refinement. *Math. Comput.*, 260:1743–1769, 2007.

3. A. Buffa and R. Hiptmair. Galerkin boundary element methods for electromagnetic scattering, extended version withe new appendix on scattering from coated dielectric objects. Technical report, http://www.sam.math.ethz.ch/ hiptmair/Courses/CEM/BUH03.pdf, Draft version, December 12, 2007.

4. K. Cools, F.P. Andriulli, D. De Zutter, and E. Michielssen. Accurate and conforming mixed discretization of the MFIE. *IEEE Antennas and Wireless Propagation Letters*, 10:528–531, 2011.

5. Anne Greenbaum and Zdenek Strakos. Any nonincreasing convergence curve is possible for GMRES. *SIAM J. Matrix Anal. Appl*, 17:465–469, 1996.

6. B.H. Jung, T.K. Sarkar, and Y.-S. Chung. A survey of various frequency domain integral equations of the analysis of scattering from three-dimensional dielectric objects. Technical report, Electrical Engineering and Computer Science, 2002. SURFACE, Paper 65.

7. B.H. Jung, T.K. Sarkar, S.W. Ting, Y. Zhang, Z. Mei, Z. Ji, M. Yuan, A. De, M. Salazar-Palma, and S.M. Rao. *Time and Frequency Domain Solutions of EM Problems Using Integral Equations and a Hybrid Metholy*. John Wiley & Sons, Inc, 2010.

8. L.C.Trintinalia and H. Ling. First order triangular patch basis functions for electromagnetic scattering analysis. *Journal of Electromagnetic Waves and Applications*, 15(11):1521–1537, 2001.

9. A. I. Mackenzie, S. M. Rao, and M. E. Baginski. Electromagnetic scattering from arbitrarily shaped dielectric bodies using paired pulse vector basis functions and method of moments. *IEEE Transactions on Antennas and Propagation*, 57(7):2076–2083, 2009.

10. J.R. Mautz and R.F. Harrington. Electromagnetic scattering from a homogenenous body of revolution. Technical Report CR-1999-209724, Department of Electrical and Computer Engineering, Syracuse University, 1999.

11. C. Müller. *Foundations of the Mathematical Theory of Electromagnetic Waves*. Springer, 1969.

12. P.Ylä-Oijala, S.P. Kiminski, K. Cools, F.P. Andriulli, and S. Järvenpää. Mixed discretization schemes for electromagnetic surface integral equations. *International Journal of Numerical Modelling: Electronic Networks, Devices and Fields*, 25:525–540, 2012.

13. P.Ylä-Oijala and M. Taskinen. Application of combined field integral equation for electromagnetic scattering by dielectric and composite objects. *IEEE Transactions on Antennas and Propagation*, 53(3):1168–1173, 2005.

14. Su Yan, Jian-Ming Jin, and Zaoping Nie. Improving the accuracy of the second kind Fredholm integral equations by using the Buffa-Christiansen functions. *IEEE Trans. Ant. Prop.*, 59(4):1299–1310, 2011.

15. Pasi Ylä-Oijala. Application of a novel CFIE for electromagnetic scattering by dielectric objects. *Microwave and Opt. Tech. Letters*, 35:3–5, 2002.

16. Pasi Ylä-Oijala, Matti Taskinen, and S. Järvenpää. Surface integral equation formulations for solving electromagnetic scattering problems with iterative methods. *Radio Science*, 40(6), 2005.